PCCP

Accepted Manuscript

ROYAL SOCIETY OF CHEMISTRY

www.rsc.org/pccp

The role of substrate structure in the on-surface synthesis of organometallic and covalent oligophenylene chains

Jingya Dai[a], Qitang Fan[a], Tao Wang[a], Julian Kuttner[b], Gerhard Hilt[b], J. Michael Gottfried*[b], Junfa Zhu*[a]

Influences of the substrate structure on the formation of one-dimensional organometallic and covalent oligomers on a Cu(110) surface were studied with scanning tunneling microscopy (STM), X-ray photoemission spectroscopy (XPS), and low energy electron diffraction (LEED) in ultrahigh vacuum (UHV). Vapor deposition of submonolayer 4,4''-dibromo-*meta*-terphenyl (DMTP) onto Cu(110) at 300 K leads to scission of C-Br bonds and the formation of organometallic chains (*cis*/*trans* and all-*trans*) connected by C-Cu-C bonds. Larger islands (120 x 120 nm^2) of all-*trans* zigzag organometallic chains as sole products were obtained by deposition of DMTP onto Cu(110) held at 383 K. The domains are oriented along two directions with an angle of ±13° relative to the [0 0 1] direction due to the two-fold symmetry of the Cu(110) surface lattice. This study reveals at a sub-molecular level that the organometallic chains firstly lose copper atoms and then undergo C-C coupling into oligophenylene chains at a substrate temperature around 417 K. Annealing the large islands of organometallic chains to 458 K results in the formation of completely C-C covalent bonded zigzag oligophenylene chains. The zigzag angle of 125° slightly deviates from the ideal value of 120°. This is attributed to a stretching of the zigzag oligophenylene chains due to substrate template effects.

1. Introduction

Polymerization of functional molecular tectons into complex molecular networks directly on surfaces is an effective route to synthesize robust one- and two-dimensional (1D/2D) molecular architectures, which have great potential for applications in molecular electronics, catalysis, gas storage, magnetism and other fields.[1-11] A key challenge is the controlled assembly of molecules into desired architectures connected by organometallic or covalent bonds, which are often thermally more stable than van der Waals or hydrogen bonds.[12-16] The Ullmann reaction,[17-18] a C-C coupling reaction between haloarenes induced by metal, has been employed extensively on metal surfaces to build nanowires,[19-23] nanoribbons,[3, 21, 24-28] or covalent organic networks.[1, 16, 29-32] According to previous research in this field, the surface assisted Ullmann reaction starts with the scission of the carbon-halogen bond, leading to the formation of intermediate organometallic nanostructures connected by C-Cu-C bonds. The coupled Cu atoms are released when the structures are annealed to a higher temperature resulting in the formation of covalent organic nanostructures.[33] The formation of organometallic and covalent nanostructures is typically influenced by both the precursor monomer and the substrate, and also by the halogen by-products. A typical method for obtaining covalent nanostructures with enhanced structural uniformity and compactness is to provide a low coupling probability by a deliberate selection of precursor and substrate.[34] However, only few works have studied the effect of commensurability (i.e., the lattice match between the formed covalent nanostructures and substrate lattice) on the formation of the final covalent species.[20, 35] A recent example is the lattice directed formation of covalent or organometallic wires from 2,5-diethynyl-1,4-bis(phenylethynyl)-benzene on different lattice planes of single-crystalline silver.[36] The substrate commensurability was also reported to be a significant factor in surface-assisted coordination chemistry. For instance, trimesic acid (TMA) underwent deprotonation and assembled into $[Cu(tma)_4]^{n-}$ tetramer arrays on the Cu(100) surface.[37] However, it formed one-dimensional coordination chains on the Cu(110) surface.[38] In another system, the stability and structure of the pyridyl-Cu-pyridyl coordination

[a] National Synchrotron Radiation Laboratory and Collaborative Innovation Center of Suzhou Nano Science and Technology, University of Science and Technology of China, Hefei, 230029, P.R. China, jfzhu@ustc.edu.cn

[b] Fachbereich Chemie, Philipps-Universität Marburg, Hans-Meerwein-Str., 35032 Marburg, Germany, michael.gottfried@chemie.uni-marburg.de

chains were strongly affected by their commensurability with the substrate.[39]

In our previous work,[40] well-defined six-fold symmetric hyperbenzene arrays were obtained as major product after deposition of 4,4''-dibromo-*meta*-terphenyl (DMTP) onto the Cu(111) surface (three-fold symmetric) at 550 K (scheme 1, pathway 2).[41] As a side product, zigzag oligophenylene chains were obtained with only limited yield. This raises the question how the balance between the hexagonal hyperbenzene rings and the zigzag chains, which have two-fold rotational symmetry, can be influenced by substrate template effects. Therefore, we choose a two-fold symmetric Cu(110) surface as the substrate in this study, and expect to obtain two-fold symmetric oligophenylene chains (scheme 1, pathway 1) as the major product from DMTP molecules, according to commensurability and symmetry matching considerations. The detailed step-by-step reactions of DMTP on Cu(110) were studied by ultrahigh vacuum (UHV) scanning tunneling microscopy (STM), low energy electron diffraction (LEED) and X-ray photoelectron spectroscopy (XPS). Comparison between Cu(110) and Cu(111) shows that the substrate structure influences the selectivity for the formation of organometallic and covalent products. Due to the two-fold symmetry and anisotropy of Cu(110), no cyclic organometallic and covalent species were observed on this surface, in contrast to the findings for Cu(111). These results strongly imply that the surface Ullmann reaction and its products can be effectively steered by the substrate lattice.

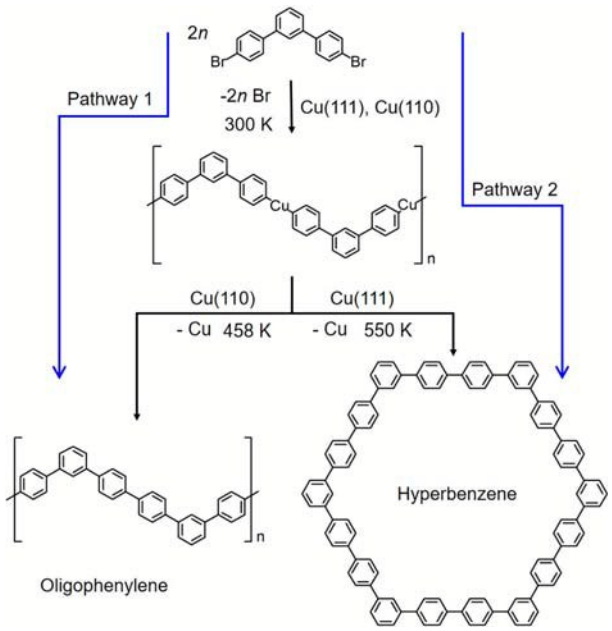

Scheme 1. Major reaction pathways for 4,4''-dibromo-*meta*-terphenyl (DMTP) on Cu(110) and Cu(111) surfaces.

2. Experimental Section

The experiments were performed in a two-chamber ultrahigh vacuum (UHV) system, which has been described previously,[42] at a background pressure below 10^{-10} mbar. Briefly, the system comprises a hemispherical analyzer for XPS, a twin-anode X-ray source (SPECS), retractable four-grid LEED optics (SPECS ErLEED), a quadrapole mass spectrometer and a scanning tunneling microscope (SPECS STM 150 Aarhus). For STM, all voltages refer to the sample and the images were recorded in constant current mode at a sample temperature of 300 K. Moderate filtering (Gaussian smooth, background subtraction) has been applied using the WSxM software.[43] The Cu(110) single crystal was purchased from MaTecK, Germany, with an alignment of better than 0.1° with respect to the nominal orientation. Preparation of a clean and structurally well controlled Cu(110) surface was achieved by cycles of bombardment with Ar^+ ions and annealing at 850 K. 4,4''-dibromo-1,1':3',1''-terphenyl (4,4''-dibromo-*meta*-terphenyl, DMTP) was made from 4-bromophenylacetylene in a short reaction sequence utilizing a Grubbs-enyne metathesis reaction and a regioselective cobalt-catalyzed Diels-Alder reaction followed by mild oxidation, as described previously.[41] DMTP was vapor-deposited from a Kentax evaporator with a quartz crucible held at 369 K. The deposition rate of DMTP was about 0.12 ML per minute (unless indicated otherwise). Coverages were derived from STM images and XPS measurements.

3. Results and discussion

Small islands with limited degree of order were obtained after deposition of 0.48 ML DMTP onto Cu(110) at 300 K, as shown in Figure 1a. According to our previous studies of DMTP and other aromatic halides on the Cu(111) surface,[22, 33, 44] C-Br bonds undergo dissociation at (and well below) 300 K, resulting in the formation of *meta*-terphenyl (MTP) fragments. Since the Cu(110) surface is generally even more reactive than the Cu(111) surface, C-Br bond dissociation is expected to occur on Cu(110) at 300 K as well. This is also evidenced by the Br 3p XP spectrum shown in Figure S1. In the gas phase, these fragments would be biradicals, but on the copper surface, the former Br positions are most likely occupied by Cu adatoms, as

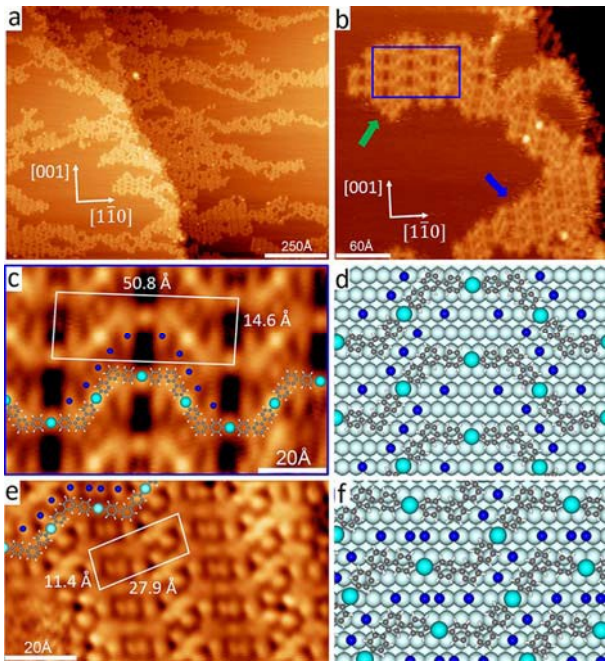

Figure 1. a) Overview STM image recorded at 300 K after 0.48 ML DMTP molecules were deposited onto Cu(110) at 300 K. Tunneling conditions: U = -2.9 V, I = 0.02 nA. b) Zoom-in STM image of (a) showing two kinds of islands marked by green and blue arrows, U = -2.9 V, I = 0.02 nA. c) Magnified view of the blue framed region in (b) showing the *cis*/*trans* chains, U = -2.9 V, I = 0.03 nA. d) Adsorption model of the molecular structure in (c) for the *cis*/*trans* configured chains. e) High resolution STM image of a section of the same all-*trans* zigzag structure as marked by blue arrow in (b), U = -2.0 V, I = 0.02 nA. f) Adsorption model of the molecular structure in (d) for the all-*trans* zigzag chains. Color code: C, gray; H, white; Br, blue; coupling Cu atoms, cyan; Cu(110) lattice, powder-blue.

reported previously.[44] In Figure 1b, which shows a magnified section of Figure 1a, two kinds of chain islands can be observed: Zigzag chains with all-*trans* configuration (blue arrow) and chains with alternating *cis*/*trans* configuration (green arrow). Both types of chains are composed of bent units (*meta*-terphenyl (MTP) units, i.e., the debrominated precursor molecules) linked by bright protrusions (Cu adatoms), which can be easily identified by the high-resolution STM images shown in Figure 1c and 1e, respectively, and the overlaid molecular models. According to the high-resolution STM images, the molecular models for *cis*/*trans* configured chains and all-*trans* zigzag chains are established as shown in Figure 1d and 1f, respectively. Apparently, these two structures differ in the adsorption configuration of the MTP units in their unit-cells. The *cis*/*trans* organometallic chains consist of MTP units with four adsorption configurations oriented towards two directions. However, the MTP units in all-*trans* zigzag organometallic chains have only two adsorption configurations, which are oriented along the same direction. The lattice constant along the all-*trans* zigzag chains is 27.9 ± 0.2 Å. This is larger than the lattice constant for direct C-C linkage (21.8 Å)[41] and thus consistent with the formation of C-Cu-C bonds between the MTP units. Moreover, the periodic protrusions in the centers of the straight parts along the chains are another piece of evidence for the existence of coupling Cu atoms. It is worth noting that one of the coupling Cu atoms in an unit-cell is brighter than the other one, which can be ascribed to the different adsorption sites, as reported previously for DMTP on Cu(111).[44]

In Figure 1f, the Cu atoms in the C-Cu-C units alternatingly occupy hollow and bridge sites, which leads to the alternating bright and dark protrusions between the bends. Noteworthy, the lattice constant of 27.9 ± 0.2 Å along the all-*trans* zigzag chains is slightly larger than on the Cu(111) surface (26.5 Å).[41] This is mainly due to the fact that the C-Cu bond adapts its length in order to reach commensurability between the formed zigzag chains and the Cu(110) surface. According to the the high-resolution STM images and adsorption model, a matrix of this commensurable zigzag organometallic chains relative to the Cu(110) surface lattice is derived to be (-1, 3| 3, 10). The spot-like protrusions between the all-*trans* zigzag organometallic chains (Figure 1e) are assigned to chemisorbed Br atoms resulting from the dissociation of the C-Br bonds upon deposition of DMTP onto Cu(110). These Br related features have been observed and reported previously.[22, 33, 44] According to the structural model in Figure 1f, all Br adatoms are adsorbed at the short bridge sites on the Cu(110) surface. The large lattice constant perpendicular to the chains (11.4 ± 0.1 Å for the all-*trans* zigzag chains, 14.6 ± 0.1 Å for the *cis*/*trans* chains) shows the absence of covalent bonds between the chains, which suggests that the assembly of zigzag chains to islands may be driven by hydrogen bonds between Br adatoms and H atoms of MTP units. A similar case has been reported previously for 9,10-dibromoanthracene on the Ag(111) surface,[45] where Br···H bonds play a vital role to mediate the conformation of organometallic chains.

Deposition of an increased coverage of DMTP precursors (0.84 ML) onto the Cu(110) surface at 300 K leads to the formation of an increased number of small organometallic chain islands which dispersively distribute on the surface, as shown in Figure 2a. However, after deposition of the same coverage (0.84 ML)

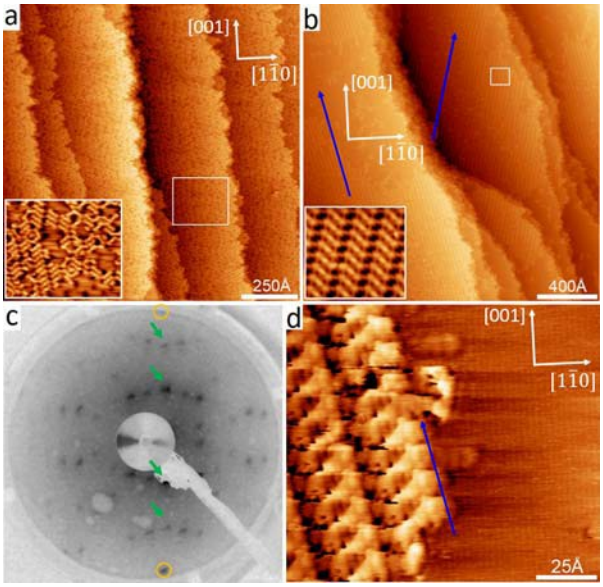

Figure 2. a) Overview STM image after deposition of 0.84 ML DMTP molecules onto Cu(110) held at 300 K, U = 0.14 V, I = 0.1 nA. Inset shows the zoom-in of the white framed region. b) Overview STM image obtained after deposition of 0.84 ML DMTP molecules onto Cu(110) held at 383K, U = 1.9 V, I = 0.08 nA. Inset shows the zoom-in of the white framed region. c) Experimental LEED pattern for the sample in (b) (E_{el} = 20 eV). d) A section of zigzag organometallic chain island with substrate lattice resolved, U = 0.8 V, I = 0.09 nA. All STM images were recorded at 300 K.

of DMTP onto Cu(110) held at 383 K, larger islands with defect-free areas of up to 120 × 120 nm^2 are formed, as shown in Figure 2b. Moreover, only all-*trans* zigzag organometallic chain islands (no *cis*/*trans* chains) are observed on the terraces. This suggests that the all-*trans* zigzag organometallic chains are thermodynamically more stable than the *cis*/*trans* chains. In contrast to six orientations of the formed organometallic chain domains on Cu(111) surface,[44] the organometallic chain islands here (on Cu(110)) have only two mirrored domains relative to the [001] direction, as shown by the two blue arrows in Figure 2b. In addition, no single organometallic loops or back-folding of the chains at the boundary of islands can be observed, in contrast to those frequently found on the Cu(111) surface.[44] Since the major difference between Cu(111) and Cu(110) surface lies in the different symmetries of their lattices. The case on Cu(111) indicates that the six orientations of the formed organometallic chains and formation of organometallic loops requires the template assistance of the three-fold symmetric Cu(111) substrate lattice. On that surface, the MTP units adsorb with twelve optimal configurations oriented along six equivalent directions.[41] This favors the formation of loops and back-folding of the organometallic chains. In contrast, here on the two-fold symmetric anisotropic Cu(110) surface, the four adsorption configurations of the terphenyl units are oriented along the two mirrored directions and thus cannot form a back-folding motif.

The commensurability between the all-*trans* zigzag organometallic chain islands and the substrate is corroborated by the LEED pattern shown in Figure 2c, which contains spots derived from two domain orientations of equivalent symmetry. This is in very good agreement with a simulated LEED pattern (Figure S2) described by the epitaxy matrices (-1, 3| 3, 10) and (1, 3| -3, 10), which correspond well with the unit cells of the two domains observed by STM (Figure 1e). The dots marked by orange circles indicate the 1 × 1 spots of the substrate lattice. The spots marked by green arrows indicate a triple periodicity (relative to the substrate lattice) for the all-*trans* zigzag organometallic chains along the [0 0 1] direction, which agrees very well with the adsorption model shown in Figure 1f. In addition, the relative angle between the orientation of the chain islands (blue arrow in Figure 2d) and the [0 0 1] direction of Cu(110) is 13.7 ± 0.5°, according to the STM image shown in Figure 2d, where both the zigzag organometallic chains and the substrate are atomically resolved. This agrees very well with the calculated value (13.3°) from the proposed adsorption model (Figure 1f) and the experimental LEED pattern (14.0 ± 0.9°).

Figure 3a shows the overview STM image acquired after deposition of 0.48 ML DMTP onto the Cu(110) surface, which was held at 383 K during the deposition. Many of the all-*trans* zigzag organometallic chain islands have a straight boundary edge along the direction perpendicular to the chains, such as indicated by the green line in Figure 3a. Figure 3b shows the magnified view of the organometallic chain island in Figure 3a (compare the position of the green line). Figure 3b reveals that the island boundary passes through the copper atoms located at hollow sites (the weaker protrusions in organometallic chains). This means that the freely diffusing MTP units on the terraces prefer to stick to the copper atom adsorbed at a short bridge sites in a preformed organometallic chain. Previous findings for Cu(111) indicate that the organometallic zigzag chains form islands which are very elongated in the direction of the chains.[44] This is not the case on Cu(110), where the islands have more square shape, suggesting that the growth rate is similar in both directions along and vertical to the chain.

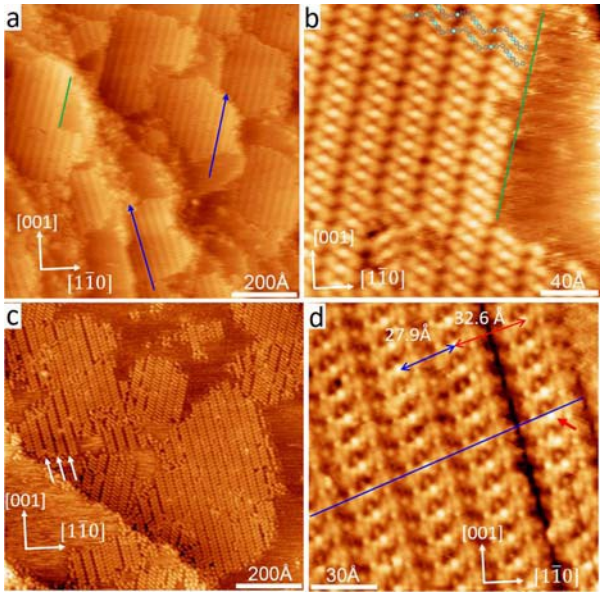

Figure 3. a) Overview STM image obtained after deposition of 0.48 ML DMTP molecules onto Cu(110) held at 383 K , U = 2.9 V, I = 0.06 nA. b) Magnified view of the all-*trans* zigzag organometallic chain islands in Figure 3a, U = 2.9 V, I = 0.06 nA, with overlaid model in the upper part. c) Overview STM image obtained after deposition of 0.48 ML DMTP onto Cu(110) held at 407 K , U = -1.2 V, I = 0.03 nA. The white arrows mark the split line defects. d) Magnified view of the all-*trans* zigzag organometallic chain island of the sample in (c) in which a split defect can be seen, U = -0.9 V, I = 0.04 nA. See the text for the meaning of the lines and the red arrow.

After deposition of the same coverage of DMTP onto the Cu(110) surface held at a higher temperature (407 K), partial splitting of the all-*trans* zigzag chains is observed, as shown by Figure 3c (marked with white arrows). Figure 3d shows the high-resolution STM image of a region with such a split defect, which appears as a dark line almost perpendicular to the chains. The STM contrast is in agreement with the elimination of Cu atoms from the C-Cu-C bonds. This is further evidenced by the distance between two neighboring equivalent Cu atoms located on different sides of the line defect (32.6 ± 0.2 Å, marked with red line in Figure 3d). This value is much larger than the lattice constant along zigzag organometallic chains (27.9 ± 0.2 Å, shown by blue line in Figure 3d), which proves the absence of C-Cu-C bonds between the zigzag chains in the left and the right part of the split line defect. Furthermore, the MTP-Cu-MTP dimers at the right side of the defect are dislocated relative to the main body of the island (on the left side of the line defect). As indicated by the blue line in Figure 3d, the coupling Cu atom marked by the red arrow are not located on the same line as the Cu atoms on the left of the line defect, i.e., the translational symmetry is interrupted in both directions. This again strongly suggests that the C-Cu-C bonds with Cu atoms adsorbed at hollow sites are relatively weaker than those with Cu atoms at short bridge sites.

Figure 4a shows a section of a sub-molecularly resolved STM

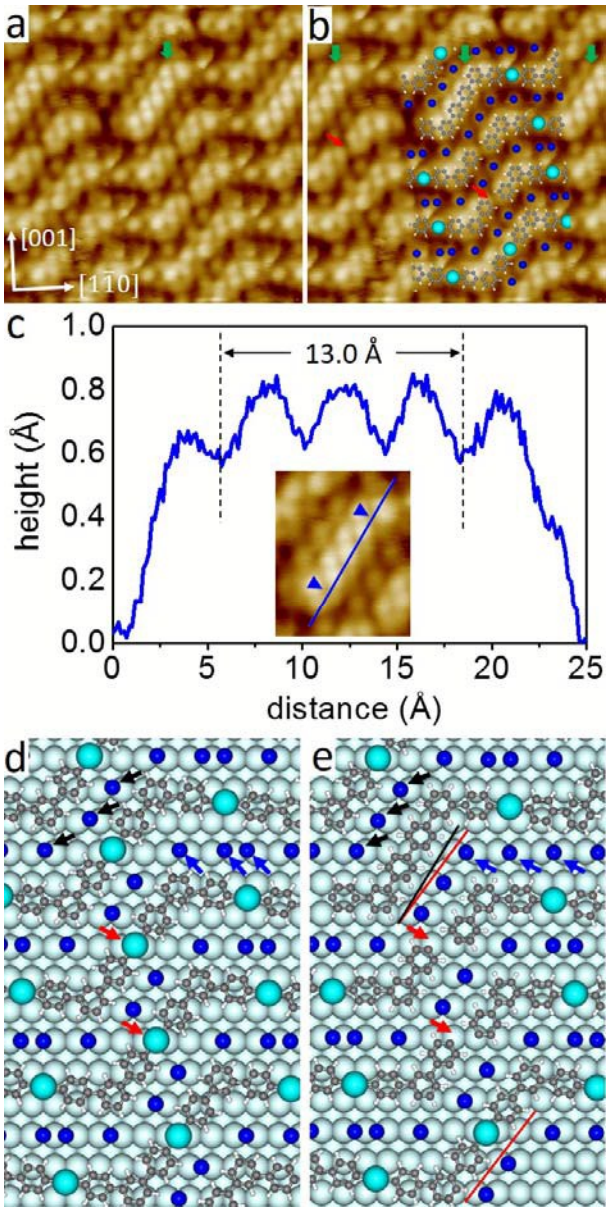

Figure 4. a) STM image with sub-molecular resolution obtained after deposition of 0.48 ML DMTP onto Cu(110) held at 417 K, U = 0.3 V, I = 0.08 nA. b) Molecular model partially superimposed on (a). c) Apparent height profile along the straight line in the inset (oligophenylene unit marked by green arrow in panel (a)) from bottom to top. d) A section of the proposed model in Figure 1f for the defect-free zigzag organometallic chain island. e) Proposed adsorption model of the selected region in panel (b). See the text for the meaning of the lines and arrows.

image of the sample after deposition of 0.48 ML DMTP onto Cu(110) held at 417 K. Since the loss of Cu from the C-Cu-C bonds already occurs at the substrate temperature of 407 K, the subsequent C-C coupling process is expected to happen at this or slightly higher temperatures. This is confirmed by Figure 4a and 4b: The positions where Cu atoms have disappeared from the C-Cu-C links are marked by red arrows (see also the overlaid molecular model in Figure 4b). In addition, the formation of new C-C covalent bonds (marked by green arrows in Figure 4b) between MTP units can be observed. The occurrence of C-C coupling in the islands of the organometallic chain reveals the evolution process from organometallic chains to covalent oligomers. These C-C coupling events take place preferentially after eliminating Cu atoms adsorbed at the short bridged sites. This suggests that the energy barrier for the transformation from C-Cu-C bonds to C-C bonds is lower when the bridging Cu atoms were adsorbed at short bridge sites, compared to bridging Cu atoms at the hollow sites, although the elimination of coupling Cu atoms can be observed at both short bridge and hollow sites.

The formation of C-C bonds was directly evidenced by the submolecularly resolved STM image shown in Figure 4a. Four phenyl rings can be resolved in the straight part of the oligophenylene units as marked by the green arrow in Figure 4a. As shown by the apparent height profile along the blue line in Figure 4c, the distance between two neighboring minima, which corresponds to two centers of the phenyl rings, of the curve is measured to be (13.0 ± 0.5/3) Å = 4.3 ± 0.2 Å, which agrees very well with the distance of two phenyl units in the phenylene chains as reported previously to be 4.4 ± 0.2 Å.[18] These segments can be viewed as the early stage of the final covalently bonded oligophenylene zigzag chains. Note that the occurrence of C-C coupling between two MTP units also influences the adjacent MTP units in the remaining organometallic chains. Figure 4e shows the detailed adsorption model of the selected region in Figure 4b (the region overlaid with molecular model), which was derived based on the high-resolution STM image in Figure 4a. By comparison with Figure 4d, the adsorption model of a section of ideal zigzag organometallic chains, reaction-induced changes of the adsorption configuration are revealed. On the one hand, the loss of the coupling Cu atoms in the C-Cu-C bonds changes the azimuthal orientation of the MTP units, as shown by the black and red lines in Figure 4e. This is mainly due to the shrinking of the chain length when the C-Cu-C bonds turn into C-C bonds. The products assume a new stable adsorption configuration with optimized registry on the substrate. The remaining free radicals of the MTP units after elimination of the coupled Cu atoms are tentatively proposed to bind to the vicinal substrate Cu atoms as indicated by the red arrows in Figure 4e. On the other hand, the occasionally observed C-C coupling in the organometallic chains results in the dislocation of adjacent Br atoms as marked by two groups of arrows (black and blue) in Figure 4d and 4e. Nevertheless, the preferred adsorption sites of the Br adatoms, the short bridge sites, remain the same. The dislocation of the Br atoms most likely results from the Br···H bonds to the hydrogen atoms at the periphery of the MTP units.

Annealing the sample in Figure 2b to a higher temperature of 458 K leads to the formation of a rather disordered phase of short zigzag chains and other features, as shown in Figure 5a. The zigzag chains here are characterized by a uniform apparent height, which contrasts the non-uniform height of the zigzag organometallic chains formed below 383 K. The disappearance of highly ordered organometallic chain domains and the uniform height suggest that the bridging Cu atoms are released from the C-Cu-C links and that the newly formed short chains are now connected by C-C bonds, as will be discussed in detail

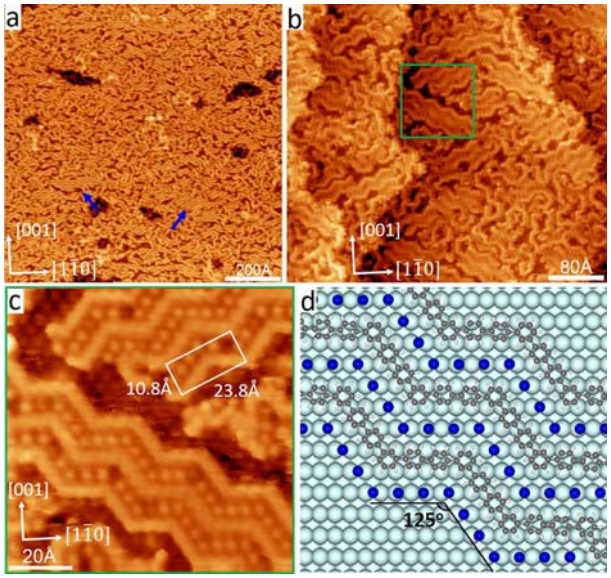

Figure 5. a) Overview STM image taken after annealing the sample in Figure 2b to 458 K, U = 2.0 V, I = 0.06 nA. b) Higher resolution STM image of the as-prepared sample in panel (a), U = -0.7 V, I = 0.04 nA. c) Zoom-in STM image of the green framed region in (b), U = -1.5 V, I = 0.06 nA. d) Detailed adsorption model of zigzag oligophenylene chains.

below. Most of the MTP units are connected with each other

to form irregular motifs, except for some small islands consisting of zigzag oligophenylene chains, as marked by the blue arrows in Figure 5a. Hyperbenzene or other cyclic species that were formed on Cu(111) under similar conditions[41] are not observed on Cu(110). The selectivity for chain formation is attributed to the commensurability between the formed C-C covalent species and the two-fold symmetry of the Cu(110) substrate.

Figure 5b shows a higher resolution STM image of the zigzag oligophenylene chains. The additional dot-like protrusions, which fill up the regions between the zigzag chains, are attributed to Br adatoms, according to previous works.[44] The unit cell of these zigzag chain islands is (10.8 ± 0.1 Å) × (23.8 ± 0.3) Å as shown by the white rectangle in Figure 5c. The lattice constant along the chain direction here is only 23.8 ± 0.3 Å, compared to 27.9 ± 0.2 Å for the all-*trans* zigzag organometallic chains. The observed contraction and the more uniform apparent height of short zigzag chains strongly indicate the formation of C-C bonds (rather than C-Cu-C bonds) between MTP units, that is, the formation of oligo-phenylene chains. The distance between the two adjacent zigzag oligophenylene chains is 10.8 ± 0.1 Å, which agrees very well with the distance between the zigzag organometallic chains (11.4 ± 0.1 Å) in Figure 1e. Thus, similar to that in organometallic chains, the Br adatoms between the chains function as "adhesive" to stabilize two adjacent oligophenylene chains. Figure 5b also shows irregular links, i.e., links by which the MTP units are not only connected at the terminal positions. This indicates that the formation of C-C bonds from C-Cu-C bridges competes with the activation of C-H bonds.

Notably, the newly formed zigzag oligophenylene chains are stretched along the chain direction. Figure 5d shows the adsorption model of a section of zigzag oligophenylene chains, based on the high-resolution STM image in Figure 5c. The clearly resolved Br adatoms between the zigzag chains help to determine an unambiguous adsorption model, taking into account the distance between Br adatoms and the direction of the Br adatom arrays. Thus, the angle of the bend (between two adjacent straight phenylene fragments) of the zigzag chains is calculated to be 125° (in alignment with the measured 125 ± 1°), which is slightly larger than the ideal value of 120°. The stretching of zigzag chains can also be evidenced by the larger lattice constant of 23.8 ± 0.3 Å than that observed on the Cu(111) surface (21.8 Å), whereas the distance between the chains is almost the same (10.7 Å on Cu(111)).[41] The stretching is most likely driven by adsorbate-substrate interactions and results in a better commensurability with the surface lattice. The energy necessary for the deformation of the MTP units may be a significant factor that limits the length of the zigzag oligophenylene chains, which on average contain only five MTP units, compared to ten units on Cu(111).[41] Therefore, the substrate structure greatly influences the growth of C-C covalent bonded nanostructures, especially regarding the selectivity for the final products.

4. Conclusion

When 4,4''-dibromo-*meta*-terphenyl (DMTP) is deposited onto Cu(110) surface at 300 K, the C-Br bonds dissociate immediately. The resulting *meta*-terphenyl (MTP) fragments form two kinds of organometallic chains, i.e., the *cis/trans* and the all-*trans* zigzag organometallic chains. The lengths of the repeat units along the chain directions are 50.8 ± 0.3 Å and 27.9 ± 0.2 Å, respectively. Both chains form small islands, in which the residual Br adatoms are adsorbed at the short bridge sites between the chains. The Cu atoms in the C-Cu-C bonds of the all-*trans* organometallic chains alternatingly occupy hollow sites and short bridge sites along the chains. Deposition of DMTP at 383 K leads to the formation of larger islands of the all-*trans* zigzag organometallic chains, while the *cis*/*trans* organometallic chains vanish. This reveals that the former are thermodynamically more stable. The islands of all-*trans* zigzag organometallic chains are oriented along two directions, which enclose angles of ±13° relative to the [0 0 1] direction of the Cu(110) lattice. Deposition of DMTP at 407 K results in the partial splitting of the all-*trans* zigzag chains by elimination of Cu from some of the C-Cu-C bonds. Following the loss of Cu from the C-Cu-C bonds, C-C bond formation starts within the all-*trans* zigzag organometallic chains at 417 K. Small islands that exclusively consist of zigzag oligophenylene chain occur after annealing the all-*trans* zigzag organometallic chains to 458 K. The zigzag angles of 125° are larger than the ideal 120° angle, indicating that the chains are stretched along the chains direction. Accordingly, the lattice constant along the chains is 23.8 ± 0.3 Å, compared to 21.8 Å reported for the unstretched chains on Cu(111). The stretching is apparently necessary for the system to achieve commensurability between the chains, the Br atoms on the short bridge sites between the chains, and the substrate. The fact that large islands of all-*trans* zigzag

organometallic chains, but only small islands of zigzag oligophenylene chains are formed is mainly attributed to their different commensurability with the substrate lattice. No hyperbenzene or other larger hydrocarbon macrocycles are observed on the Cu(110) surface, contrasting previous observations on Cu(111). These results illustrate how the symmetry and structure of the substrate affect the formation of ordered organometallic and covalent structures.

Acknowledgements

J.F.Z. acknowledges the financial support from the National Basic Research Program of China (2013CB834605), the National Natural Science Foundation of China (Grant No.21173200 and 21473178), and the Scientific Research and Users with Potential Grants of Hefei Science Center of CAS (2015SRG-HSC031, 2015HSC-UP022). J.M.G. thanks the Deutsche Forschungsgemeinschaft (DFG) for support through SFB 1083 and grant GO 1812/2-1 and the Chinese Academy of Sciences for a Visiting Professorship for Senior International Scientists (Grant No. 2011T2J33).

Notes and references

1. L. Grill, M. Dyer, L. Lafferentz, M. Persson, M. V. Peters and S. Hecht, *Nat. Nanotechnol.*, 2007, **2**, 687-691.
2. L. Lafferentz, V. Eberhardt, C. Dri, C. Africh, G. Comelli, F. Esch, S. Hecht and L. Grill, *Nat. Chem.*, 2012, **4**, 215-220.
3. J. Cai, P. Ruffieux, R. Jaafar, M. Bieri, T. Braun, S. Blankenburg, M. Muoth, A. P. Seitsonen, M. Saleh, X. Feng, K. Muellen and R. Fasel, *Nature,* 2010, **466**, 470-473.
4. M. Treier, C. A. Pignedoli, T. Laino, R. Rieger, K. Müllen, D. Passerone and R. Fasel, *Nat. Chem.,* 2011, **3**, 61-67.
5. C. A. Palma and P. Samori, *Nat. Chem.,* 2011, **3**, 431-436.
6. J. V. Barth, G. Costantini, K. Kern, *Nature*, 2005, **437**, 671-679.
7. H. W. Langmi, J. W. Ren, B. North, M. Mathe and D. Bessarabov, Electrochimica *Acta* 2014, **128**, 368-392.
8. J. Lee, O. K. Farha, J. Roberts, K. A. Scheidt, S. T. Nguyen and J. T. Hupp, *Soc. Rev.,* 2009, **38**, 1450-1459.
9. L. J. Murray, M. Dinca and J. R. Long, *Soc. Rev.,* 2009, **38**, 1294-1314.
10. M. Kurmoo, *Chem. Soc. Rev.,* 2009, **38**, 1353-1379.
11. A. Nitzan and M. A. Ratner, *Science*, 2003, **300**, 1384-1389.
12. D. Heim, D. Ecija, K. Seutert, W. Auwärter, C. Aurisicchio, C. Fabbro, D. Bonifazi and J. V. Barth, *J. Am. Chem. Soc.,* 2010, **132**, 6783-6790.
13. S. Haq, F. Hanke, M. S. Dyer, M. Persson, P. Iavicoli, D. B. Amabilino and R. Raval, *J. Am. Chem. Soc.*, 2011, **133**, 12031-12039.
14. Z. L. Shi and N. Lin, *J. Am. Chem. Soc.,* 2009, **131**, 5376-5377.
15. Q. Li, J. R. Owens, C. B. Han, B. G. Sumpter, W. C. Lu, J. Bernholc, V. Meunier, P. Maksymovych, M. Fuentes-Cabrera and M. H. Pan, *Sci. Rep.,* 2013, **3**, 2102.
16. M. Bieri, M. T. Nguyen, O. Groning, J. M. Cai, M. Treier, K. Ait-Mansour, P. Ruffieux, C. A. Pignedoli, D. Passerone, M. Kastler, K. Mullen and R. Fasel, *J. Am. Chem. Soc.,* 2010, **132**, 16669-16676.
17. F. Ullmann and J. Bielecki, *Ber. Deutsch. Chem. Ges.,* 1901, **34**, 2174-2185.
18. M. Di Giovannantonio, M. El Garah, J. Lipton-Duffin, V. Meunier, L. Cardenas, Y. Fagot Revurat, A. Cossaro, A. Verdini, D. F. Perepichka, F. Rosei and G. Contini, *ACS Nano,* 2013, **7**, 8190-8198.
19. L. Lafferentz, F. Ample, H. Yu, S. Hecht, C. Joachim and L.Grill, *Science*, 2009, **323**, 1193-1197.
20. J. A. Lipton-Duffin, O. Ivasenko, D. F. Perepichka and F. Rosei, *Small*, 2009, **5**, 592-597.
21. A. Basagni, F. Sedona, C. A. Pignedoli, M. Cattelan, L. Nicolas, M. Casarin and M. Sambi, *J. Am. Chem. Soc.,* 2015, **137**, 1802-1808.
22. W. H. Wang, X. Q. Shi, S. Y. Wang, M. A. Van Hove and N. Lin, *J. Am. Chem. Soc.,* 2011, **133**, 13264-13267.
23. G. Vasseur, Y. Fagot-Revurat, M. Sicot, B. Kierren, L. Moreau, D. Malterre, L. Cardenas, G. Galeotti, J. Lipton-Duffin, F. Rosei, M. Di Giovannantonio, G. Contini, P. Le Fevre, F. Bertran, L. Liang, V. Meunier and D.F. Perepichka, *Nat. Commun.*, 2016, **7**, 10235.
24. S. Blankenburg, J. Cai, P. Ruffieux, R. Jaafar, D. Passerone, X. Feng, K. Müllen, R. Fasel and C. A. Pignedoli, *ACS Nano,* 2012, **6**, 2020-2025.
25. K. A. Simonov, N. A. Vinogradov, A. S. Vinogradov, A. V. Generalov, E. M. Zagrebina, G. I. Svirskiy, A. A. Cafolla, T. Carpy, J. P. Cunniffe, T. Taketsugu, A. Lyalin, N. Martensson and A. B. Preobrajenski, *ACS Nano*, 2015, **9**, 8997−9011.
26. J. Cai , C. A. Pignedoli, L. Talirz, P. Ruffieux, H. Söde, L. Liang, V. Meunier, R. Berger, R. Li and X. Feng, *Nat. Nanotechnol.,* 2014, **9**, 896-900.
27. P. Han, K. Akagi, F. Federici Canova, H. Mutoh, S. Shiraki, K. Iwaya, P. S. Weiss, N. Asao and T. Hitosugi, *ACS Nano,* 2014, **8**, 9181-9187.

28. H. Zhang, H. Lin, K. Sun, L. Chen, Y. Zagranyarski, N. Aghdassi, S. Duhm, Q. Li, D. Zhong, Y. Li, K. Mullen, H. Fuchs and L. Chi. *J. Am. Chem. Soc.,* 2015, **137**, 4022−4025.
29. M. Bieri, M. Treier, J. Cai, K. Ait-Mansour, P. Ruffieux, O. Groning, P. Groning, M. Kastler, R. Rieger, X. Feng, K. Mullen and R. Fasel, *Chem. Commun.,* 2009, **45,** 6919-6921.
30. J. Eichhorn, D. Nieckarz, O. Ochs, D. Samanta, M. Schmittel, P. J. Szabelski and M. Lackinger, *ACS Nano*, 2014, **8**, 7880-7889.
31. J. Eichhorn, T. Strunskus, A. Rastgoo-Lahrood, D. Samanta, M. Schmittel and M. Lackinger, *Chem. commun.,* 2014, **50**, 7680-7682.
32. M. Bieri, S. Blankenburg, M. Kivala, C. A. Pignedoli, P. Ruffieux, K. Mullen and R. Fasel, *Chem. Commun.,* 2011, **47**, 10239-10241.
33. Q. Fan, C. Wang, L. Liu, Y. Han, J. Zhao, J. Zhu, J. Kuttner, G. Hilt and J. M. Gottfried, *J. Phys. Chem. C,* 2014, **118**, 13018-13025.
34. Q. Fan, J. M. Gottfried and J. Zhu, *Account. Chem. Res.,* 2015, **48**, 2484-2494.
35. K. A. Simonov, N. A. Vinogradov, A. S. Vinogradov, A. V. Generalov, E. M. Zagrebina, G. I. Svirskiy, A. A. Cafolla, T. Carpy, J. P. Cunniffe, T. Taketsugu, A. Lyalin, N. Martensson and A. B. Preobrajenski, *ACS Nano,* 2015, **9**, 8997-9011.
36. J. Liu, Q. Chen, L. Xiao, J. Shang, X. Zhou, Y. Zhang, Y. Wang, X. Shao, J. Li, W. Chen, G. Q. Xu, H. Tang, D. Zhao and K. Wu, *ACS Nano,* 2015, **9**, 6305-6314.
37. N. Lin, A. Dmitriev, J. Weckesser, J. V. Barth and K. Kern, *Angew. Chem., Int. Ed.,* 2002, **41**, 4779-4783.
38. T. Classen, G. Fratesi, G. Costantini, S. Fabris, F. L. Stadler, C. Kim, S. de Gironcoli, S. Baroni and K. Kern, *Angew. Chem., Int. Ed.,* 2005, **44**, 6142-6145.
39. S. L. Tait, A. Langner, N. Lin, S. Stepanow, C. Rajadurai, M. Ruben and K. Kern, *J. Phys. Chem. C,* 2007, **111**, 10982-10987.
40. Q. Fan, J. Dai, T. Wang, J. Kuttner, G. Hilt, J. M. Gottfried and J. Zhu, *ACS Nano*, 2016, **10**, 3747-3754.
41. Q. Fan, C. Wang, Y. Han, J. Zhu, W. Hieringer, J. Kuttner, G. Hilt and J. M. Gottfried, *Angew. Chem., Int. Ed.,* 2013, **52**, 4668-4672.
42. M. Chen, X. F. Feng, L. Zhang, H. X. Ju, Q. Xu, J. F. Zhu, J. M. Gottfried, K. Ibrahim, H. J. Qian and J. O. Wang, *J. Phys. Chem. C,* 2010, **114**, 9908-9916.
43. I. Horcas, R. Fernandez, J. M. Gomez-Rodriguez, J. Colchero, J. Gomez-Herrero and A. M. Baro, *Rev. Sci. Instrum.,* 2007, **78**, 013705.
44. Q. Fan, C. Wang, Y. Han, J. Zhu, J. Kuttner, G. Hilt and J. M. Gottfried, *ACS Nano,* 2014, **8**, 709-718.
45. J. Park, K. Y. Kim, K.-H. Chung, J. K. Yoon, H. Kim, S. Han and S.-J. Kahng, J. Phys. Chem. C., 2011, **115**, 14834-14838.